

# Harnessing Deep Learning and HPC Kernels via High-Level Loop and Tensor Abstractions on CPU Architectures

Evangelos Georganas\*, Dhiraj Kalamkar\*, Kirill Voronin\*, Antonio Noack#, Hans Pabst\*, Alexander Breuer#, Alexander Heinecke\*

\*Intel Corporation

#Friedrich-Schiller-Universität Jena

## ABSTRACT

During the past decade, Deep Learning (DL) algorithms, programming systems and hardware have converged with the High Performance Computing (HPC) counterparts. Nevertheless, the programming methodology of DL and HPC systems is stagnant, relying on highly-optimized, yet platform-specific and inflexible vendor-optimized libraries. Such libraries provide close-to-peak performance on specific platforms, kernels and shapes thereof that vendors have dedicated optimizations efforts, while they underperform in the remaining use-cases, yielding non-portable codes with performance glass-jaws. This work introduces a framework to develop efficient, portable DL and HPC kernels for modern CPU architectures. We decompose the kernel development in two steps: 1) Expressing the computational core using Tensor Processing Primitives (TPPs): a compact, versatile set of 2D-tensor operators, 2) Expressing the logical loops around TPPs in a high-level, declarative fashion whereas the exact instantiation (ordering, tiling, parallelization) is determined via simple knobs. We demonstrate the efficacy of our approach using standalone kernels and end-to-end workloads that outperform state-of-the-art implementations on diverse CPU platforms.

## 1 INTRODUCTION

Deep Learning (DL) emerged as a promising machine learning paradigm more than a decade ago, and since then, deep neural networks have made significant advancements in various fields, including computer vision, natural language processing, and recommender systems, while gradually expanding their applications in traditional scientific domains [1–10]. These DL workloads exhibit diverse computational characteristics and demands, owing to the wide range of problems they address. Despite the apparent differences between conventional High Performance Computing (HPC) and DL workloads, the computational kernels used in both fields largely overlap. These kernels involve tensor contractions (dense and sparse), elementwise tensor operations, tensor norm computations, and generalized tensor re-orderings [11, 12].

The deployment of programming systems, algorithms, and hardware in the domain of DL has led to convergence with the HPC counterparts. However, the prevalent programming paradigm has become stagnant compared to the rapidly evolving DL/HPC workloads. The programming paradigm relies heavily on vendor-optimized libraries for vital building blocks of applications. These libraries offer close-to-peak performance on specific platforms, kernels, and shapes thereof that vendors have dedicated optimization efforts towards. However, they under-perform in other use-cases, resulting in non-portable, inflexible codes with performance limitations. Meanwhile, mainstream CPU platforms have continued to evolve,

offering hardware acceleration capabilities for key operations, core heterogeneity, large core-counts, and complex memory hierarchies. The aforementioned nuances of contemporary CPU platforms make it impractical to use "one-fits-all" code generation strategies, exacerbating the generalization problem inherited by extended library dependencies. Consequently, this complexity is transferred to library development, and libraries for key computations become highly specialized, making them difficult to develop, maintain, and extend to encompass the latest CPU advances [13]. In the quest of eliminating the dependency from vendor-libraries, the research fields of Tensor Compilers (e.g. [14–17]) and Domain Specific Languages (DSLs) (e.g. [18, 19]) are experiencing a renaissance. Nevertheless, such effort typically provide point solutions (often domain specific), and have not proven their applicability on real-world use-case scenarios [13].

We observe that the root cause of the aforementioned problems can be traced back to the extreme abstraction levels provided by libraries and tensor compilers. The libraries are characterized by coarse-grain, monolithic kernels that lack flexibility, while compilers allow for unrestricted expression of low-level operators, which can hinder efficient code generation in the back-ends. Adding to the difficulty of achieving optimal code generation, tensor compilers are responsible for efficiently parallelizing, tiling, and re-ordering loops, as well as transforming the layout of data structures. All these tasks remain unsolved in a generic setup to date. These observations suggest that a middle path that embraces high-level abstractions for the loop generation and the tensor operations, and emphasizes clear separation of concerns can effectively tackle the majority of the challenges [13].

In this study we built upon and extend the prior work of Georganas et.al. [12], namely Tensor Processing Primitives (TPP). TPPs comprise a collection of basic operators on 2D tensors that can be used to construct more complex operations on high-dimensional tensors. The TPP collection is compact, expressive, and precision-aware, and as a result high-level DL and HPC kernels can be written in terms of TPP operations. The specification for TPPs is agnostic to platform, DL framework, and compiler back-end, which makes the TPP-code portable. TPPs operate at the sub-tensor granularity, making them directly accessible to workload and library developers. While the TPP specification is platform-agnostic, its implementation is platform-specific, and optimized for the target architectures. This separation of concerns allows the user-entirety of TPPs to focus on the algorithm and its execution schedules, while the TPP back-end generates efficient, platform-specific code for the TPP operations. TPPs could be also viewed as a "virtual Tensor ISA" that abstracts the actual physical ISA of the target.

While the TPP abstraction addresses the code generation problem of the core computation kernels, it is still the user-entity’s responsibility to write the required nested loops around the TPP primitives (henceforth called “outer loops”) that essentially traverse the computation/iteration space of the kernel. These “outer loops” effectively control the parallelization scheme of the computation, and the corresponding loop orders in conjunction with potential loop blockings/tilings affect the temporal and spatial locality of the computation [20, 21]. Consequently, in order to get high-performance kernels, the user has to write (potentially) complicated, non-portable (across platforms) code with respect to these “outer loops” that takes into account the increasingly complex memory hierarchy of the diverse compute platform, and the increased degree of available parallelism. Also, the exact instantiation of these loops that yields optimal kernel performance directly depends on the problem size and the platform at hand (i.e. there is no “one-fits-all” solution, an issue that also hinders portable library performance).

We address the problem of generating arbitrarily complex parallel loops around TPPs by introducing PARLOOPER (PARallel LOOP gEneratoR), a high-level loop abstraction framework. PARLOOPER aims to simplify the “outer loop” writing by enabling the user to declare the logical “outer loops” along with their specifications (i.e. bounds/steps/parallelization properties), instead of having to explicitly write the tedious loop nests involving multiple loop orders, tilings and parallelization schemes. At runtime, the user may provide a single parameter (henceforth called *loop-instantiation knob*) to dictate the desired instantiation of the loop nest (i.e. loop order, loop blockings/tilings, parallelization method). In our Proof-Of-Concept (POC) implementation, PARLOOPER is a lightweight C++ library that auto-generates Just-In-Time (JIT) the requested instantiation of the loop nest by considering the loop specifications and the single *loop-instantiation knob* runtime parameter. The resulting user’s code is extremely simple, declarative, and high-level yet powerful: With zero lines of code-changes the loop nest can be instantiated to arbitrarily complex implementation that maximizes the performance for a specific platform and problem at hand. PARLOOPER uses internally caching schemes to avoid JIT overheads whenever possible. By leveraging PARLOOPER along with the TPP programming abstraction for the core computation, the user code is simple/declarative, and naturally lends itself to auto-tuning to explore complex outer loop instantiations with zero lines of user-code writing. This allows for efficient implementation of loop nests/tensor computations with skewed sizes whereas libraries usually ill-behave.

By combining PARLOOPER (high-level loop abstraction) and TPP (high-level tensor-operation abstraction) we get a framework to develop efficient, portable DL and HPC kernels for modern CPU architectures. We decompose the kernel development in two steps with clear separation of concerns. First, we express the computational core/body of a kernel using solely Tensor Processing Primitives and the *logical* loop indices of the surrounding/“outer” loops. Second, we declare the surrounding *logical* loops along with their specification (i.e. bounds/steps/parallelization properties) with PARLOOPER. The result is a streamlined, compact code that is identical for all target platforms/problem sizes/shapes; the exact instantiation of the loop-nest is governed by a simple runtime knob, whereas

the efficient code generation pertaining to TPP is undertaken by the TPP back-end which is JITting code based on the target platform.

The *loop-instantiation knob* in PARLOOPER can be determined either “manually” by the user (i.e. the user a priori selects values for the knob that yield good performance based on custom performance modeling) or by auto-tuning techniques, where a bunch of values for the *loop-instantiation knob* are benchmarked offline and the best one is selected during runtime. To assist the selection of the loop-instantiation runtime knob, instead of relying exclusively on manual settings/exhaustive auto-tuning, we provide an exemplary lightweight, high-level performance modeling tool. This tool takes as input the abstract loop order along with a *loop-instantiation knob*, the computational core expressed via tensor-contraction TPPs, and few parameters modeling the target CPU architecture, and it simulates/predicts the performance of a specific setup. As a result, one can do offline, cross-architecture loop-tunings based on this tool and obtain a set of good loop-instantiation knobs that can be further refined via auto-tuning or can be used opportunistically during runtime.

We demonstrate the efficiency of our approach on multiple platforms using standalone kernels written with this methodology and compare the performance to vendor-optimized libraries. Finally, we showcase the expressiveness and viability of our methodology by implementing contemporary end-to-end DL workloads using solely the TPP and PARLOOPER abstractions and show how we can outperform the state-of-the-art implementations on multiple CPU platforms. The main contributions of this work are:

- A lightweight, flexible and high-level parallel loop generation framework (PARLOOPER) that decouples the logical loop declaration from the actual nested loop instantiation (i.e. loop ordering, loop tiling, parallelization). The user-code is written at high-level by merely declaring the logical loops, whereas the exact instantiation is controlled by a single knob.
- Extending the LIBXSMM TPP backend to support the ARM SVE ISA and hardware accelerated tensor-contractions on the Graviton 3 architecture. Also, we introduce sparse  $\times$  dense matrix multiplication TPPs with block sparsity, low-precision support and hardware acceleration for both x86 and ARM/AArch64 platforms.
- Implementing exemplary DL and HPC multi-threaded kernels using the PARLOOPER framework and the TPP abstraction for the core computations (GEMM, convolutions, MLP, block-sparse  $\times$  dense GEMM) including multiple precisions.
- Implementing end-to-end DL workloads via the PARLOOPER/TPP paradigm for Image Recognition (ResNet50 [22]) and Large Language Model (BERT [23]) pipelines.
- Exemplary auto-tuning infrastructure for kernels written with the PARLOOPER/TPP framework. We also construct a high-level simulator that models the performance of nested loops with tensor contractions on various platforms, allowing cross-platform and offline tuning of the abstract loops.
- Benchmarking the standalone kernels and end-to-end workloads on multiple modern CPU architectures with varying ISAs, concurrency levels, HW acceleration capabilities and memory hierarchies (servers and client parts, heterogeneous cores) with various datatype precisions while matching/exceeding state-of-the-art (SOTA) performance from vendor-optimized libraries.

```

1 DType A[Mb][Kb][bk][bm]; //Block M dim with bm and K dim with bk
2 DType B[Nb][Kb][bn][bk]; //Block N dim with bn and K dim with bk
3 DType C[Nb][Mb][bn][bm]; //Block N dim with bn and M dim with bm
4
5 auto gemm_loop = ThreadedLoop<3>({
6   LoopSpecs{0, Kb, k_step, {l1_k_step, l0_k_step}}, // K-loop "a"
7   LoopSpecs{0, Mb, m_step, {l1_m_step, l0_m_step}}, // M-loop "b"
8   LoopSpecs{0, Nb, n_step, {l1_n_step, l0_n_step}}, // N-loop "c"
9   loop_spec_string;
10
11 gemm_loop(
12   [&](int* ind) {
13     int ik = ind[0], im = ind[1], in = ind[2];
14     unsigned long long brcount = k_step;
15     if (ik == 0) zero_tpp( &C[ind][im][0][0] );
16     brgemm_tpp( &A[ind][ik][0], &B[ind][ik][0][0], &C[ind][im][0][0],
17               &brcount );
18   });

```

**Listing 1: GEMM written with PARLOOPER and TPPs**

Section 2 details the design and implementation of the PARLOOPER framework along with the POC performance modeling tool. Then, Sections 3 and 4 illustrate the exemplary implementation of HPC and DL kernels, and end-to-end workloads using the PARLOOPER/TPP paradigm. Section 5 presents an experimental evaluation of the aforementioned DL and HPC kernels/workloads on multiple CPU platforms. Sections 6 and 7 summarize the related work and conclude this paper.

## 2 THE PARLOOPER FRAMEWORK

The development of kernels via PARLOOPER consists of two steps:

- (1) Declaring the logical loops along with their specification
- (2) Expressing the computation using the logical indices of the loops

We will illustrate these two steps with a simple General Matrix Multiplication (GEMM) example, and our desired computation will be expressed by leveraging exclusively Tensor Processing Primitives (TPP). The TPPs we are going to use are the *zero\_tpp* and the *brgemm\_tpp*. The *zero\_tpp* merely sets the input 2D tensor to zero values. The *brgemm\_tpp* corresponds to the *Batch-Reduce GEMM* (BRGEMM) TPP which is the main building block for general tensor contractions in the TPP collection [12, 21]. BRGEMM materializes the operation  $C = \beta \cdot C + \sum_{i=0}^{brcount-1} A_i \times B_i$ . In essence, this kernel multiplies the specified blocks  $A_i^{bm \times bk}$  and  $B_i^{bk \times bn}$  and reduces the partial results to a block  $C^{bm \times bn}$ . In this example we use the *stride-based* variant of BRGEMM, where the addresses of  $A_i$  and  $B_i$  are:  $address_{A_i} = address_{A_{i-1}} + stride_A$  and  $address_{B_i} = address_{B_{i-1}} + stride_B$  [12].

The Matrix Multiplication input tensors are logically 2D matrices  $A^{M \times K}$  and  $B^{K \times N}$  that need to be multiplied and added onto  $C^{M \times N}$ . To maximize performance, we follow the approach of previous work [21] and we block the dimensions  $M$ ,  $K$ , and  $N$  by factors  $bm$ ,  $bk$ , and  $bn$  respectively (lines 1-3 of Listing 1). We employ the BRGEMM TPP in order to perform the tensor contraction with  $A$  and  $B$  across their dimensions  $Kb$  and  $bk$  (which constitute the  $K$ /inner-product dimension of the original 2D matrices). In regard to the stride-based BRGEMM setup, the sub-blocks  $A_i$  and  $B_i$  that have to be multiplied and reduced are apart by fixed strides  $stride_A = bk \cdot bm$  and  $stride_B = bn \cdot bk$ .

### 2.1 Logical Loop Declaration

```

1 void parlooper_nested_loops(std::function<void(int*)> body_func,
2                             std::function<void()> init_func,
3                             std::function<void()> term_func) {
4     #pragma omp parallel
5     {
6         if (init_func) init_func();
7         for b0 = 0 to Mb with step l1_m_step
8             for c0 = 0 to Nb with step l1_n_step
9                 for a0 = 0 to Kb with step k_step
10                    #pragma omp for collapse(2) nowait
11                    for b1 = b0 to b0 + l1_m_step with step l0_m_step
12                        for c1 = c0 to c0 + l1_n_step with step n_step
13                            for b2 = b1 to b1 + l0_m_step with step m_step
14                                // Logical indices for computation are a0, b2, c1
15                                int ind[3] = {a0, b2, c1};
16                                body_func(ind);
17                            if (term_func) term_func();
18                    }
19    }

```

**Listing 2: Generated loop nest for  $loop\_spec\_string = bcaBCb$ .**

The Matrix Multiplication algorithm is comprised of three logical nested loops which are declared in lines 5-9 of Listing 1. Since our computation involves three logical loops we use in the declaration: `ThreadedLoop<3>` (line 5).

The first loop (line 6) which has the mnemonic *a*, corresponds to a loop with start 0, upper bound  $Kb$  and step  $k\_step$ , and in our use-case corresponds to the “ $K$ ” loop of the GEMM ( $K$  is the inner-product / contraction dimension). This loop has an optional list of step/blocking parameters  $\{l1\_k\_step, l0\_k\_step\}$ . The second loop (line 7) which has the mnemonic *b*, corresponds to a loop with start 0, upper bound  $Mb$  and step  $m\_step$ , and in our use-case corresponds to the “ $M$ ” loop of the GEMM (number of rows of the output tensor in column-major format). Similarly, this loop has an optional list of step/blocking parameters  $\{l1\_m\_step, l0\_m\_step\}$ . Finally, the third loop (line 8) which has the mnemonic *c*, corresponds to a loop with start 0, upper bound  $Nb$  and step  $n\_step$ , and in our use-case corresponds to the “ $N$ ” loop of the GEMM (number of columns of the output tensor in column-major format). This loop has an optional list of step/blocking parameters  $\{l1\_n\_step, l0\_n\_step\}$ .

The specific instantiation of these loops, i.e. the loop order with which they appear, the number of times each one is blocked and also the way they are parallelized are controlled by the run-time knob *loop\_spec\_string*. Given such a string during run-time, the constructor *ThreadedLoop* invokes our custom loop generator and emits a C++ function for the target loop instantiation. Listing 2 illustrates an exemplary target-loop instantiation function. Subsequently, a C++ compiler is invoked (currently we support `icc`, `clang`, and `gcc`), and the target-loop instantiation function is compiled Just-In-Time (JIT), which can be further used by the code (line 11 in Listing 1). In order to avoid JIT overheads whenever possible, we cache the JITed target loops using internal caching schemes, i.e. if we request the same loop nest with the same *loop\_spec\_string*, we merely return the function pointer of the already compiled and cached loop-nest. Subsection 2.2 provides more details with respect to the target-loop instantiation function and its API.

The two rules for constructing a valid *loop\_spec\_string* are:

- **RULE 1: Loop ordering and blockings**

Each character (from *a* to *z*, depending on the number of the logical loops) can appear in any order and any number of times. In our case, since we have 3 logical loops the characters range from *a* to *c*. The order with which the loop characters appear in

the string determine the nesting loop order, and the times each character appears determines how many times the corresponding logical loop is blocked. For example, a *loop\_spec\_string* *bcabc* corresponds to a loop where logical loop *b* is blocked twice (the character *b* appears 3 times), logical loop *c* is blocked once (the character *c* appears 2 times) and the logical loop *a* is not blocked (it appears only once). The blocking/tiling sizes for each logical loop level are extracted from the corresponding list of step/blocking parameters in order they appear in the list. Currently our Proof-Of-Concept (POC) implementation of PARLOOPER allows only perfectly nested blocking/tiling sizes, i.e. in the example above it should hold:  $l1\_m\_step \% l0\_m\_step = 0$ ,  $l0\_m\_step \% m\_step = 0$  and  $l1\_n\_step \% n\_step = 0$ . All these blocking/tiling sizes lists may be provided at runtime (e.g., programmatically determine the blocking sizes given a problem) and do not have to be statically determined.

#### • RULE 2: Parallelization of loops

If a loop character in the *loop\_spec\_string* appears in its upper-case form, it dictates the intention to parallelize this loop at the specific nest-level it appears. Following the previous example, if the *loop\_spec\_string* was *bcaBcb*, it would correspond to a loop nest where the second occurrence of loop *b* would be parallelized. Currently our implementation supports 2 modes of parallelization:

**PAR-MODE 1: Relying on OpenMP [24] runtime for parallelizing the loops.** By following this method, effectively the loop parallelization strategy corresponds to the directive `#pragma omp for nowait`. If the user intends to parallelize multiple loops, the corresponding capitalized characters should appear consecutively in the *loop\_spec\_string*, and it would result in parallelization using collapse semantics. For example, if the *loop\_spec\_string* was *bcaBCb*, PARLOOPER would generate the loop nest shown in Listing 2. We allow to specify optionally additional directives at the end of the *loop\_spec\_string* by using the special character `@` as separator. For example the loop string “*bcaBCb @ schedule(dynamic, 1)*” yields the parallelization directive: `#pragma omp for collapse(2) schedule(dynamic, 1) nowait`. This method allows PARLOOPER to leverage features from the OpenMP runtime, e.g. dynamic thread scheduling. The constructed loop nest is embraced by a `#pragma omp parallel` region (line 4 in Listing 2). In case the user desires a barrier at the end of a specific loop-level, it may be requested using the special character “|”.

**PAR-MODE 2: Using explicit multi-dimensional thread decompositions.** Using this parallelization paradigm, the user can specify explicit 1D, 2D or 3D loop parallelization schemes by parallelizing 1, 2 or 3 loops respectively. For the 1D decomposition, the threads are forming a logical  $R \times 1$  1D grid and are assigned the corresponding parallelized loop iterations in a block fashion. To apply this explicit decomposition, the user merely has to append after the desired upper-case loop character the substring `[R:#threads]`, where `#threads` is a number dictating in how many ways to parallelize that loop. For a 2D decomposition, the threads are forming a logical  $R \times C$  2D grid that effectively parallelizes the requested two loops. Unlike PAR-MODE 1 which honors collapse semantics, the parallelized loops do *not* have to appear consecutively in the *loop\_spec\_string*. For example consider the *loop\_spec\_string* *bC[R:16]aB[C:4]cb*. The loop *c0* is parallelized 16-ways and the loop *b1* is parallelized 4-ways using a logical thread grid of  $16 \times 4$  ( $R = 16$ ,  $C = 4$ ) – see Listing 3.

```

1 # pragma omp parallel
2 {
3   int tid = omp_get_thread_num();
4   int row_teams = 16, col_teams = 4;
5   int row_id = id/col_teams, col_id = tid%col_teams;
6   if (init_func) init_func();
7   for b0 = 0 to Mb with step l1_m_step
8     # Parallelize 16-ways loop c0, assign tasks based on row_id
9     for c0 = 0 to Nb with step l1_n_step
10      for a0 = 0 to Kb with step k_step
11        # Parallelize 4-ways loop b1, assign tasks based on col_id
12        for b1 = b0 to b0 + l1_m_step with step l0_m_step
13          for c1 = c0 to c0 + l1_n_step with step n_step
14            for b2 = b1 to b1 + l0_m_step with step m_step
15              // Logical indices for computation are a0, b2, c1
16              int ind[3] = {a0, b2, c1};
17              body_func(ind);
18            if (term_func) term_func();
19 }

```

**Listing 3: Loop nest for *loop\_spec\_string* = *bC{R : 16}aB{C : 4}cb***

Each loop that is parallelized is done so in a block fashion using the requested number of “ways”. The 3D decomposition works in an analogous manner, where the threads are forming a logical  $R \times C \times L$  3D grid.

Even though in the current incarnation of PARLOOPER we support only the OpenMP runtime for concurrency purposes, our backend loop generator can be trivially extended to support other runtimes (e.g. Threaded Building Blocks (TBB) [25] or pthreads [26]).

## 2.2 Expressing the Computation

After the desired nested loop has been declared/specified, we get back an initialized ThreadedLoop object (the *gemm\_loop* object in Line 5 of Listing 1) which can be passed at runtime (up to) three parameters:

- (Optional) A pointer to a function with signature: **`void init_func()`** This function is called just before the generated loop-nest and can be used for “initialization code” purposes (e.g., code that would initialize some data structures etc.).
- (Optional) A pointer to a function with signature: **`void term_func()`** This function is called just after the generated loop-nest and can be used for “termination code” purposes (e.g., code that would clean-up some data structures etc).
- A pointer to a function with signature: **`void body_func(int *ind)`**

The function *body\_func* is called at the inner-most level of the generated loop-nest (line 16 in Listing 2), and essentially it will perform the desired computation. The function *body\_func* gets as input an array of integer values which contains in the first *N* locations the values of the logical indices used in the nested loop in alphabetical order. In essence *ind[0]* corresponds to the value of the logical index *a* in the current nested-loop iteration, *ind[1]* corresponds to the value of the logical index *b* in the current nested-loop iteration etc. This index array is automatically allocated and initialized by PARLOOPER (line 15 in Listing 2). By leveraging the values of the logical indices, the user can express the desired computation as a function of those. For convenience, we use as *body\_func* an in-place C++ lambda expression, but this is not a requirement in our framework. Considering the GEMM example above, and using lambda expression for *body\_func* we can express the desired GEMM computation using the *zero\_tpp*, the *brgemm\_tpp*,

and the logical indices with lines 12-17 of Listing 1. In line 13, we extract the logical indices  $ik$ ,  $im$  and  $in$  from the input array  $ind$ . We set batch-reduce count in Line 14 to  $k\_step$  since the tensor contraction is performed on blocked matrices. In Line 15 we set the current  $C_{in,im}$  block to zero if this is the first time we encounter it. Finally, lines 16-17 execute the actual tensor contraction via the BRGEMM TPP:  $C = \beta \cdot C + \sum_{i=0}^{brcount-1} A_i \times B_i$  for the blocks corresponding to the logical tensor slices  $A_{im,ik}$  and  $B_{in,ik}$  of the current loop-nest iteration.

At this point we want to highlight the separation of concerns which lies in the heart of PARLOOPER’s design philosophy: The logical loops are declared at a high-level by the user in as little as 3 lines of code (lines 6-8 in Listing 1). The main computational core is orthogonal to the loop declaration and is expressed via TPPs in 5 lines of code by making use only of the *logical* loop indices. Both the loop-nest instantiation and the TPP implementation are abstracted from the user and are determined at run-time considering proper knobs (e.g. *loop\_spec\_string* for the loop generation and the target platform for the code generation of the TPP). For example, on a CPU platform with 3 levels of cache and for large input tensors one may want to block each of the logical loops up to 3 times with proper block factors to maximize the data re-use out of each level of cache [27]. Moreover, skewed tensor sizes may favor loop orders where the “smaller” tensor is accessed repeatedly in the innermost loop. The parallelization of the relevant  $M$  and  $N$  loops also affects the data locality and the degree of data-sharing among cores. On architectures where “neighboring” cores share some level of cache, explicit parallelization of the loops to have neighboring cores access the same tensor slices will benefit performance (due to the fact that those accesses will be served by the same cache). All these loop-instantiation decisions are completely determined via the runtime knob *loop\_spec\_string* as pointed out in Subsection 2.1. In a similar fashion, the JITed code for the BRGEMM TPP depends on the target platform. For example, on Intel Sapphire Rapids the BF16 TPP backend can emit Advanced Matrix eXtension (AMX) instructions to accelerate the tensor contractions, whereas on an AMD Zen4 platform the TPP backend can emit AVX512 BF16 FMA instructions for acceleration. All these low-level details are completely abstracted from the user-level code.

The GEMM in Listing 1 is *data-type agnostic*. All tensors have templated datatype, and the TPPs are *precision-aware* per design: depending on how they are setup, they operate with any supported datatype internally. Therefore, the same code works for all precisions without any change. Based on the datatype width one may have to adapt the loop blocking, yet this decision is abstracted from the user-code.

### 2.3 Auto-tuning the nested loops

From the previous description it is evident that a proper value of *loop\_spec\_string* is essential in order to obtain the best performance on a given combination of problem size and CPU architecture. One way to select *loop\_spec\_string* is to hand-craft specific loop strings that are expected to be performant given custom performance modeling of the given platform/problem. An alternative path towards optimal performance is *auto-tuning*. Given a logical loop declaration, along with its specifications (i.e. loop bounds and steps), the

tunable parameters one has to decide on are: (i) How many times to block each logical loops, (ii) What are the relevant blocking sizes, (iii) Which loops to parallelize, and (iv) In which order to arrange the loops once decisions (i)-(iii) are made. A key observation is that all these decisions can be mapped in 1-on-1 fashion to a specific *loop\_spec\_string* along with a list of block sizes. We created an infrastructure to auto-generate an exhaustive list of strings that observe a set of constraints.

Considering the GEMM in Listing 1 and the decisions (i)-(iv) to be made, one can specify the following set of constraints/rules:

- (1) Block loop  $a$  up to 2 times, and loops  $b$  and  $c$  up to 3 times. This should capture multi-level cache hierarchies on modern CPUs.
- (2) For each *logical* loop  $i$ , consider its logical trip count  $T_i$  and find the prime factorization of  $T_i = p_0 \cdot p_1 \cdot \dots \cdot p_n$ . Then pick as block factors the prefix products of the prime factors with the loop’s steps. For example, for the  $M$  loop (logical loop  $b$ ) we can select as  $l0\_m\_step = m\_step \cdot p_0$  and  $l1\_m\_step = l0\_m\_step \cdot p_1 = m\_step \cdot p_0 \cdot p_1$ . This is just one exemplary way to pick the blocking factors programmatically.
- (3) We can decide to parallelize (or not) the  $M$  ( $b$ ) and the  $N$  ( $c$ ) logical loops as those define independent tasks in the GEMM. We can parallelize *any* of the blocked occurrence of the  $M/N$  loops since they also constitute independent iterations.
- (4) Given a valid string stemming from rules/constraints 1-3, consider all possible character permutations.

With such a set of constraints, we generate a set of *loop\_spec\_strings*/configurations and autotune off-line based on those. We implemented this infrastructure using custom bash scripts, but it could use other well-established tools like Open-tuner [28]. This auto-tuning process involves 0 lines of code change in the GEMM user-code which remains the same as the one in Listing 1; all different loop variants dictated by the values of *loop\_spec\_strings* are auto-generated and JITed by the PARLOOPER back-end.

### 2.4 Performance modeling of generated loops

To assist the selection of the loop-instantiation *loop\_spec\_string* knob, instead of relying exclusively on manual settings/exhaustive auto-tuning, we designed a lightweight, high-level performance modeling tool. This tool takes as inputs the logical loop order along with a candidate *loop\_spec\_string*, the computational core expressed via tensor-contraction BRGEMM TPPs, and few parameters modeling the target CPU, and it simulates/predicts the performance of such a setup. With this tool, one can do off-line, cross-architecture loop-tunings, and obtain a set of good loop-instantiation knobs that can be further refined via auto-tuning or can be used opportunistically during runtime.

Currently the Proof-Of-Concept implementation of this tool works only for PARLOOPER-generated loops with BRGEMM TPPs within *body\_func* but is readily extensible to cover the rest of the TPP collection. The idea behind the performance modeling is rather simple: If one were to focus on the execution of a specific thread in a specific loop-instantiation with BRGEMM TPP as main computation, all the data that are accessed are logical slices of Tensors that can be characterized by the tensor-block indices. In the example of Listing 1, the corresponding slices of  $A_{im,ik}$ ,  $B_{in,ik}$  and

$C_{in,im}$  can be naturally characterized by the relevant indices. Additionally, each tensor slice has a well-defined size that is known given the problem size, data type and tensor layouts. Consequently, each thread can create a *trace* of its  $A$ ,  $B$  and  $C$  accesses that arise in chronological order as the thread proceeds with the execution of the specific loop-instantiation. These traces are rather compact since they register accesses of full tensor slices instead of individual cache-lines [29]. Therefore, running a data reuse algorithm where we simulate multilevel caches on a per-thread basis is a low-overhead operation.

We simulate up to 3 levels of caches, each having its own size and bandwidth. The replacement policy for each cache is Least Recently Used (LRU). When processing a thread’s trace access  $t_i$  in chronological order, we query if the corresponding tensor slice is in any level of its cache or if it resides in memory. Then, given a BRGEMM execution at iteration  $it$ , and knowing the memory/cache-locations of the current slices  $A_{it}$ ,  $B_{it}$  and  $C_{it}$  we can predict the execution cycles taken by BRGEMM by accounting for the relative cache bandwidths and the compute-peak of the platform at hand. Each level of cache is represented as set (to account for unique occurrences of tensor slices) and is updated based on the LRU policy as the execution progresses.

We perform this trace analysis of the threads in parallel, each thread processing a different trace at a time. In the current implementation we ignore for simplicity data-sharing, but the traces could be processed in lock-step fashion to account for common sub-tensors in shared levels of cache. Despite these simplifications, our performance modelling is able to: (i) single out loop instantiations (i.e. *loop\_spec\_strings*) with poor temporal/spatial locality, and (ii) identify parallel schedules with poor concurrency characteristics. Such inefficient *loop\_spec\_strings* are assigned a low relative score and can be considered sub-optimal. In Section 5.1 we illustrate a couple of representative examples with the performance modeling tool.

### 3 KERNELS DEVELOPED VIA PARLOOPER/TPP

#### 3.1 GEMM and Multi-Layer Perceptron (MLP)

##### 3.1.1 Extending GEMM with Activation Functions to MLP

Listing 1 illustrates a GEMM implementation that leverages PARLOOPER for the outer loop writing and TPP for the core computation. We extend this implementation to include *activation functions* after the GEMM computation, expressed via the corresponding TPPs. For instance, once a  $C_{in,im}$  tensor block has been fully computed, we can call a TPP on the computed 2D sub-block. In terms of code in the core body function, this merely translates to (assuming the activation function is Rectified Linear Unit (RELU):

```
1 if (ik == Kb-k_step) relu_tpp (&C[in][im][0][0] );
```

The GEMM kernel is used in the context of Deep Learning to implement a Fully-Connected Layer: an input activation tensor  $I$  is multiplied with a weight tensor  $W$  to yield the output activation tensor  $O = W \times I$ . A Multi-Layer Perceptrons (MLP) consists of (at least three) *fully connected* layers of neurons. Each neuron in the topology may be using a non-linear activation function (e.g. a RELU after the GEMM as shown above). MLP and Fully-Connected

Layers are ubiquitous in DL, including modern Large language Models [30] (see Section 4) and Recommendation Systems [31]. An MLP kernel within the PARLOOPER framework is just another loop around the GEMM primitive to capture the cascading GEMM. The weight tensor  $W_l$  of each layer  $l$  corresponds to the  $A$  tensor of the pertinent GEMM. Due to the cascading nature of MLP, the output matrix  $O_l$  of a layer  $l$  (tensor  $C$  in GEMM) is subsequently the input matrix  $I_{l+1}$  of the next layer  $l + 1$  (tensor  $B$  in the next GEMM).

##### 3.1.2 Extending the TPP backend with AArch64 SVE support

Aiming to increase the coverage of the platforms with our PARLOOPER/TPP infrastructure, we extend the open-source implementation of TPP in LIBXSMM [32] with support for Arm Scalable Vector Extension (SVE) ISA on AArch64 architectures [33]. In short, extending the TPP backend for a new ISA entails two parts:(i) Enhancing the LIBXSMM instruction encoder with the required SVE instructions and (ii) Implementing the TPP code-generation using the new SVE instructions/encoder. Since SVE introduces predicate registers and supports masked operations, the SVE-TPP backend code generation follows the same strategies as the AVX256/AVX512 code-paths for x86 code generation in LIBXSMM. The majority of the x86 instructions in the TPP back-end code generation have a semantically equivalent one in the SVE ISA, making the backend extension straightforward.

We highlight here our implementation of the (BR)GEMM TPP with SVE Matrix-Multiply Accumulate (MMLA) instructions which are unique to the AArch64 backend. These instructions interpret the vector registers as having packed  $x \times y$  matrices. For example, considering a 16-bit datatype (BF16) and a vector length of 256-bits (SVE256) each vector registers holds 16 elements. These 16 elements are interpreted as 2 concatenated  $2 \times 4$  matrices. In the same context the BF16-MMLA instruction multiples the  $2 \times 4$  matrix of BF16 values held in each 128-bit segment of the first source vector with the  $4 \times 2$  BF16 matrix in the corresponding segment of the second source vector. The resulting  $2 \times 2$  single-precision (FP32) matrix product occupies the corresponding 128-bit segment of the output vector. With these conventions in mind, the backend implementation for the (BR)GEMM TPP with MMLA instructions can follow a traditional 2D register blocking strategy [21] as long as the input tensors  $A$  and  $B$  are reformatted to pack  $2 \times 4$  and  $4 \times 2$  sub-tensors together. The TPP collection already provides the corresponding primitives to reformat matrices  $A$  and  $B$ . More specifically, the *VNNI formatting* TPP performs the transformation:  $[D_1][D_0] \rightarrow [D_1/\alpha][D_0][\alpha]$  and the *VNNIT formatting* TPP performs  $[D_1][D_0] \rightarrow [D_0/\alpha][D_1][\alpha]$  and for  $\alpha = 4$  and BF16 data-type we obtain the desired layouts. We also implement BRGEMM TPP on SVE with MMLA support where the  $B$  matrix is on-line packed to *VNNIT* format to support the case where the input tensor  $B$  is in regular/flat format.

#### 3.2 Convolution Kernels

For convolutions via PARLOOPER, we employ the direct convolution method that works on blocked tensors and uses the BRGEMM TPP as main contraction engine [20, 21].The input activation tensor  $I$  is convoluted with the weight tensor  $W$  to yield the output activation  $O$  tensors. The activation tensor conceptually consist of 4 dimensions: the minibatch size  $N$ , the number of feature maps  $C$

```

1 DType I[N][Cb][H][W][bc]; //Block C dim with bc
2 DType W[Kb][KCb][R][S][bc][bk]; //Block K with bk and C with bc
3 DType O[N][Kb][P][Q][bk]; //Block K dim with bk
4
5 auto conv_loop = ThreadedLoop <7>({
6   LoopSpecs{0, N, n_step}, // loop "a"
7   LoopSpecs{0, Cb, c_step}, // loop "b"
8   LoopSpecs{0, Kb, k_step}, // loop "c"
9   LoopSpecs{0, P, h_step}, // loop "d"
10  LoopSpecs{0, Q, w_step}, // loop "e"
11  LoopSpecs{0, R, r_step}, // loop "f"
12  LoopSpecs{0, S, s_step}, // loop "g"
13  loop_specs_str);
14
15 conv_loop(
16  [&](int* ind) {
17    int in = ind[0], ic = ind[1], ik = ind[2], ih = ind[3];
18    int iw = ind[4], ir = ind[5], is = ind[6];
19    unsigned long long brcount = c_step * r_step * s_step;
20    if (ic == 0 && ir == 0 && is == 0) {
21      zero_tpp(&O[in][ik][ih][iw][0]);
22    }
23    brgemm_tpp(&W[ik][ic][ir][is][0][0],
24              &I[in][ic][ih*str_h+ir][iw*str_w+is][0],
25              &O[in][ik][ih][iw][0], &brcount);
26  });

```

**Listing 4: Forward convolution with PARLOOPER and TPPs**

and the spatial dimensions  $H$  and  $W$ . We denote the input tensor dimensions with  $N, C, H$  and  $W$  while the corresponding output tensor dimensions are  $N, K, P$  and  $Q$ . The weight tensor is conceptually characterized also by 4 dimensions: the feature map dimensions  $C, K$  and the spatial dimensions  $R$  and  $S$ . We block the dimension  $C$  by a factor  $bc$  and the dimension  $K$  by a factor  $bk$  and we get the blocked tensors in lines 1-3 of Listing 4. Then, we declare with PARLOOPER the 7 logical loops that traverse the convolution iteration space in lines 5-13 of Listing 4. Finally, lines 16-25 express the convolution compute kernel in a lambda function by means of the 7 logical indices and the `brgemm_tpp`. For convolutions with  $R = S = 1$  we can setup a stride-based BRGEMM whereas for the other cases we can setup offset-based BRGEMM to further increase the kernel’s performance (i.e. the  $R$  and  $S$  loops would be folded in the BRGEMM by using offsets arrays in the BRGEMM call [12]).

This convolution implementation works for multiple precisions since the specialized code-generation is handled by the TPP backend. The back-propagation passes of Convolution layers required during training can be implemented in a similar fashion [20]. Our ResNet50 training code (Section 4.2) based on PARLOOPER and TPPs is utilizing such back-propagation kernels.

### 3.3 Block-Sparse $\times$ Dense Matrix Multiply

The Sparse  $\times$  Dense Matrix Multiplication is a kernel widely used in HPC, including linear solvers and graph analytics, and is typically referred to as SpMM [34]. The SpMM  $C = A \times B$  involves one sparse matrix  $A$  and two dense matrices  $B$  and  $C$ , and by exploiting the sparsity of  $A$  one can reduce both the bandwidth and the compute requirements of the underlying computation. In addition, by enforcing block sparsity on matrix  $A$  one can further increase the performance of the operation by having better data locality in the accesses of the sparse matrix and by leveraging low-precision/hardware acceleration available on modern CPU and GPU platforms. With the recent explosion in model sizes, and the intrinsic redundancy/sparsity of large models, a promising research vector is exploring block sparsity in DL [35, 36].

```

1 DType A_vals[NNZ]; // non-zero values of A in BCSC
2 int Acolptr[M/bm], Arowidx[NNZ/(bm*bk)] // Aux structs for A in BCSC
3 DType B[Nb][K/v][bn][v]; // B in vnni-packed format
4 DType C[Nb][M/v][bn][v]; // C in vnni-packed format
5
6 auto besc_spmm_loop = ThreadedLoop <3>({
7   LoopSpecs{0, K, k_step, {l1_k_step, l0_k_step}}, // K-loop "a"
8   LoopSpecs{0, Mb, m_step, {l1_m_step, l0_m_step}}, // M-loop "b"
9   LoopSpecs{0, Nb, n_step, {l1_n_step, l0_n_step}}, // N-loop "c"
10  loop_spec_string);
11
12 besc_spmm_loop(
13  [&](int* ind) {
14    int ik = ind[0], im = ind[1], in = ind[2];
15    if (ik == 0) zero_tpp( &C[in][((im*bm)/v)][0][((im*bm)%v) ] );
16    besc_spmm_tpp( A_vals, &Acolptr[im], Arowidx,
17                  &B[in][ik/v][0][ik*v],
18                  &C[in][((im*bm)/v)][0][((im*bm)%v) ] );
19  });

```

**Listing 5: Block-SpMM written with PARLOOPER and TPPs**

In this work, we extend the GEMM TPP to support  $A$  matrix being block sparse, while  $B$  and  $C$  matrices remain dense. Being motivated by the recent applications of block sparsity in Transformer models [36] we implement block sparse  $\times$  dense kernel with BF16 datatype to further leverage Fused Multiple-ADD (FMA) hardware acceleration on x86 and AArch64 CPU platforms. For our implementation, we extend again the open-source implementation of TPP in LIBXSMM. We enable support for  $A$  in Block Compressed Sparse Columns (BCSC) format where the block-size  $bm \times bk$  is parameterized. At a high-level, the code-generation of the microkernel works as follows: We iterate over a block row of  $A$  and for each non-empty block  $bm \times bk$ , we multiply it with the corresponding dense block  $bk \times bn$  of  $B$ . The resulting dense multiplication of  $bm \times bk$  with  $bk \times bn$  sub-blocks of  $A$  and  $B$  is leveraging traditional 2D register blocking [21] whenever possible (i.e. large values of  $bn$  and  $bm$ ) in order to hide FMA latency and maximize data-ruse from registers. Aiming to readily deploy low-precision acceleration instructions, we opt to use a *packed* format for the dense matrix  $B$  which is pre-formatted in *VNNI* layout (see lines 3-4 in Listing 5 where  $v$  is the *vnni* blocking-factor). We implement this Block Sparse  $\times$  Dense Matrix Multiplication TPP for x86 architectures with both `avx512-bf16` and `AMX-bf16` acceleration, and for AArch64 with both BF16 dot-product and BF16-MMLA instructions.

The PARLOOPER kernel in Listing 5 for the block-SpMM is similar to the regular GEMM. Lines 7-9 declare the logical loops of the sparse GEMM, while the main compute kernel now is the `besc_spmm_tpp` sketched in the previous paragraph. This TPP gets as input arguments the sparse matrix  $A$  in BCSC format (line 16) and matrices  $B$  and  $C$  are regular dense tensors. In Section 5.1 we show the performance benefits of this sparse kernel over the dense GEMM on multiple CPUs.

## 4 DL WORKLOADS VIA PARLOOPER/TPP

### 4.1 Large Language Model (BERT)

The BERT model is a bidirectional transformer pre-trained via a mixture of masked language modeling objective, and next-sentence prediction [23]. We implement the end-to-end workload using the architecture from Hugging Face transformers library [37]. We implemented four fused layers as PyTorch extensions in C++ using

```

1 bert_output_loops(
2   [&](int* ind) {
3     int nc = ind[0], s1 = ind[1], nk = ind[2];
4     if (nc == 0) {
5       copy_bias_tpp(&bias[nk], &dout[s1][nk][0]);
6     }
7     brgemm_tpp(&in[s1][nc][0][0],
8               &wt_V[nk][nc][0][0],
9               &dout[s1][nk][0][0], &Ncb);
10    if ((nc + Ncb) < Nc) continue;
11    if (p > 0) {
12      dropout_tpp(&dout[s1][nk][0][0], (void*)get_rng_state(),
13                &dout[s1][nk][0][0], &dp_mask[s1][nk][0][0]);
14    }
15    add_tpp(&dout[s1][nk][0][0], &in2[s1][nk][0][0],
16           &dout[s1][nk][0][0]);
17    if (!parallelized_on_nk && nk == (Nk - 1)) {
18      layernorm_tpp_eqn(&dout[s1][0][0][0], &gamma[0][0], &beta[0][0],
19                       &mean[s1], &var[s1], &out[s1][0][0][0]);
20    }
21  });

```

Listing 6: Bert-Output module with PARLOOPER and TPPs

PARLOOPER and TPP: *Bert-Embeddings*, *Bert-Self-Attention*, *Bert-Output/Bert-SelfOutput* and *Bert-Intermediate* layers.

In Listing 6 we show an implementation of the *Bert-Output/Bert-SelfOutput* module with PARLOOPER/TPPs. We invoke a BRGEMM TPP over blocked tensor layouts, and fuse bias TPP, dropout TPP, residual add TPPs and layernorm-equation TPPs [12] on a small 2D-block granularity to maximize the out-of-cache-reuse of tensors among subsequent operators [38, 39]. Unlike previous work [12] where the nested loops have a fixed ordering and parallelization, we abstract the specific instantiation with PARLOOPER and auto-tune them for the problem sizes of interest.

In a similar fashion, the *Bert-Self-Attention* layer consists of blocked tensor contractions, fused with scale, add, dropout and softmax TPP blocks. The *Bert-Embeddings* layer is comprised of embedded lookups, followed by layernorm and dropout TPPs. Finally, *Bert-Intermediate* layer is composed of BRGEMM TPP, cascaded by bias add and Gaussian Error Linear Unit (GELU) TPP. All these modules are implemented via the PARLOOPER/TPP paradigm and are auto-tuned for specific shapes.

## 4.2 Convolutional Neural Networks (CNN)

For ResNet-50 [22] training we integrated our PARLOOPER/TPP CNN kernels into PyTorch as extensions in C++. We followed the bottleneck architecture from the original paper [22], where the convolution layers (see Listing 4) are followed by batch-normalization layers expressed also via PARLOOPER and TPP primitives (see prior work [12] for batchnorm implementation with TPPs). For the Fully Connected Layer (Listing 1) and the Pooling layers we simply used their respective TPP implementation (also through the PyTorch C++ extensions). In Section 5.2 we show the performance of the end-to-end full ResNet-50 training pipeline.

## 5 EXPERIMENTAL RESULTS

We conduct experiments on a variety of platforms spanning machines with matrix accelerators (SPR, GVT3) to CPUs that are hybrid

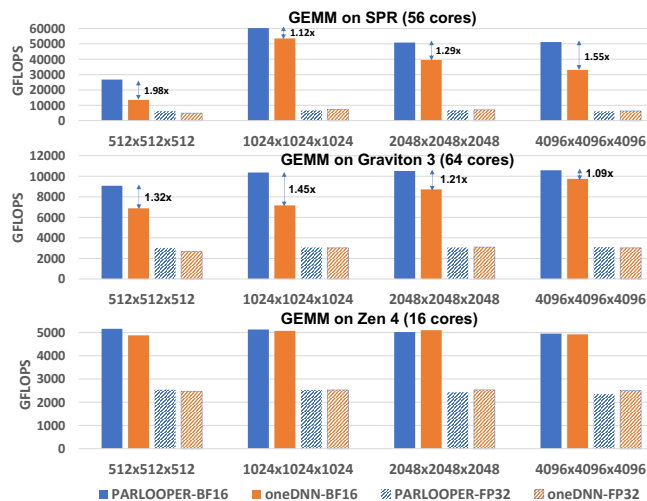


Figure 1: GEMM performance of varying sizes on (Top) SPR, (Middle) Graviton 3, and (Bottom) Zen4

and offer heterogeneous performance depending on the core-type used (ADL)<sup>1</sup>:

- SPR A dual-socket Intel Xeon 8480+ CPU and 2× 256 GB of DDR5-4800 memory with 8 channels per socket. Each CPU has 56 Golden Cove Performance cores, with AVX-512 and Intel AMX technology. Each CPU has a TDP (Thermal Design Power) of 350W.
- GVT3 A single-socket AWS Aarch64 Graviton 3 instance with 64 Neoverse V1 cores featuring SVE (256bit architecturally) incl. MMLA for matrix operations. Each socket has 8 channels of DDR5 memory and we determined through measurements that it should be DDR5-4800. The TDP per socket is not disclosed by AWS.
- Zen4 An AMD Ryzen 9 7950X desktop processor with 2-channel DDR5-6000 memory of 64 GB. The CPU features 16 of AMD Zen4 cores with support for Intel AVX-512 and has a TDP of 205W.
- ADL An Intel i9-12900K desktop processor with 2-channel DDR5-5600 memory and a capacity of 64 GB. The CPU features 8 Intel Golden Cove Performance Cores and 8 Intel Gracemont Efficiency cores and has a TDP (PL1) of 241W.

## 5.1 Standalone Kernel Performance

### 5.1.1 GEMM and MLP standalone kernels

Figure 1 shows the performance of GEMM with varying sizes ( $M \times K \times N$ ) on SPR (Top), GVT3 (Middle) and Zen4 (Bottom), for two precisions: FP32 (shaded bars) and BF16 (solid bars). The FP32 precision is representative in HPC, while the BF16 is nowadays the prevalent datatype for training/inference in production DL workloads. The blue bars correspond to our implementation with PARLOOPER/TPP, while the orange bars correspond to oneDNN [40] GEMM implementation. For GVT3 experiments with oneDNN, we enable the ARM Compute Library [41] (ACL) backend which is vendor-optimized for AArch64 platforms. At a high level we observe that

<sup>1</sup>We are not covering clock frequencies as we use the machines in turbo/unlocked (but default) configuration. Consequently, none of them have stable frequencies as they are all power limited in our tests.

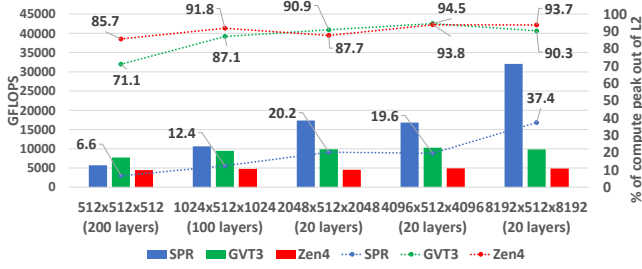


**Figure 2: MLP with Bias-Add and RELU activations with PARLOOPER/TPP.** Bars show measured performance (left y-axis), and lines show efficiency (right y-axis).

our implementation with PARLOOPER and TPPs matches/exceeds the performance of the vendor-optimized libraries. While the results for FP32 are mostly on par, for BF16 we observe speedups up to 1.98 $\times$  on SPR. The SPR experiments with BF16 datatype leverage the AMX instructions, offering up to 16 $\times$  more peak flops than the FP32 execution on AVX-512 FMA units, while have access to the same memory hierarchy. As a result, the corresponding BF16 GEMM performance is more sensitive to tensor layouts, cache blocking and microkernel efficiency, since the cache/memory subsystems is stressed more due to the higher compute peak. We note here that the oneDNN implementation does not use matrix  $B$  in blocked layout (see Listing 1) which results in extraneous cache-conflicts misses for the case with leading dimension 4096. For SPR, by leveraging BF16 and AMX we observe up to 9 $\times$  over the FP32 execution. Similar are the observations for GVT3, where our implementation outperforms oneDNN with ACL up to 1.45 $\times$  for BF16. Our newly-introduced BF16-MMLA BRGEMM kernels (Subsection 3.1.2) offer up to 3.43 $\times$  speedup over the FP32 SVE256 implementation. On Zen4, we observe that all implementations perform equally well, and the AVX-512-BF16 accelerated GEMMs observe a speedup of 2 $\times$  over the FP32 counterparts.

Figure 2 exhibits the performance of the PARLOOPER-based BF16 MLP with Bias addition and RELU activation function. We keep  $N = 512$  for these experiments, which typically corresponds to the mini-batch dimension in the DL context of MLPs, and we vary the  $M$  and  $K$  dimensions (i.e. the weight tensors of the cascading GEMMs). As we increase the weight sizes, the efficiency (dashed lines/right y-axis) keeps increasing, due to the fact that the  $B$  tensor re-use is increased. We also observe that for SPR the efficiency maxes-out at 37.4%. This is due to the cascading nature of activation tensors among layers, which causes core-to-core transfers as the activations flow from one layer to the other; in such scenarios, on SPR the LLC bandwidth is the limiting factor at scale. SPR has substantially higher compute peak than GVT3 and Zen4. Even though both the latter platforms reach more than 90% of their compute peak, the SPR platform ends up being up to 3.3 $\times$  and 6.6 $\times$  faster than GVT3 and Zen4 respectively thanks to the AMX-accelerated GEMMs.

### 5.1.2 Performance modelling of GEMM

Figure 3 shows the correlation of modeling/measured results of a  $2k \times 2k \times 2k$  GEMM on SPR (Left) and Zen4(Right) for various loops schedules/ $loop\_spec\_strings$  (see Section 2.4). The blue line

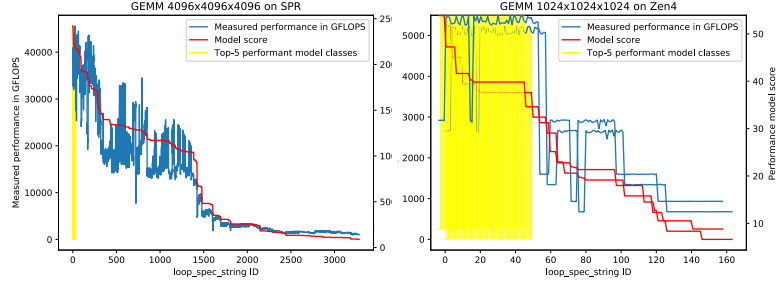


**Figure 3: Performance modeling of a  $2k \times 2k \times 2k$  GEMM on SPR (Left) and Zen4(Right)**

ID	C	K	H	W	R	S	str	ID	C	K	H	W	R	S	str
1	3	64	224	224	7	7	2	11	512	1024	28	28	1	1	2
2	64	256	56	56	1	1	1	12	512	256	28	28	1	1	2
3	64	64	56	56	1	1	1	13	256	256	14	14	3	3	1
4	64	64	56	56	3	3	1	14	256	1024	14	14	1	1	1
5	256	64	56	56	1	1	1	15	1024	256	14	14	1	1	1
6	256	512	56	56	1	1	2	16	1024	2048	14	14	1	1	2
7	256	128	56	56	1	1	2	17	1024	512	14	14	1	1	2
8	128	128	28	28	3	3	1	18	512	512	7	7	3	3	1
9	128	512	28	28	1	1	1	19	512	2048	7	7	1	1	1
10	512	128	28	28	1	1	1	20	2048	512	7	7	1	1	1

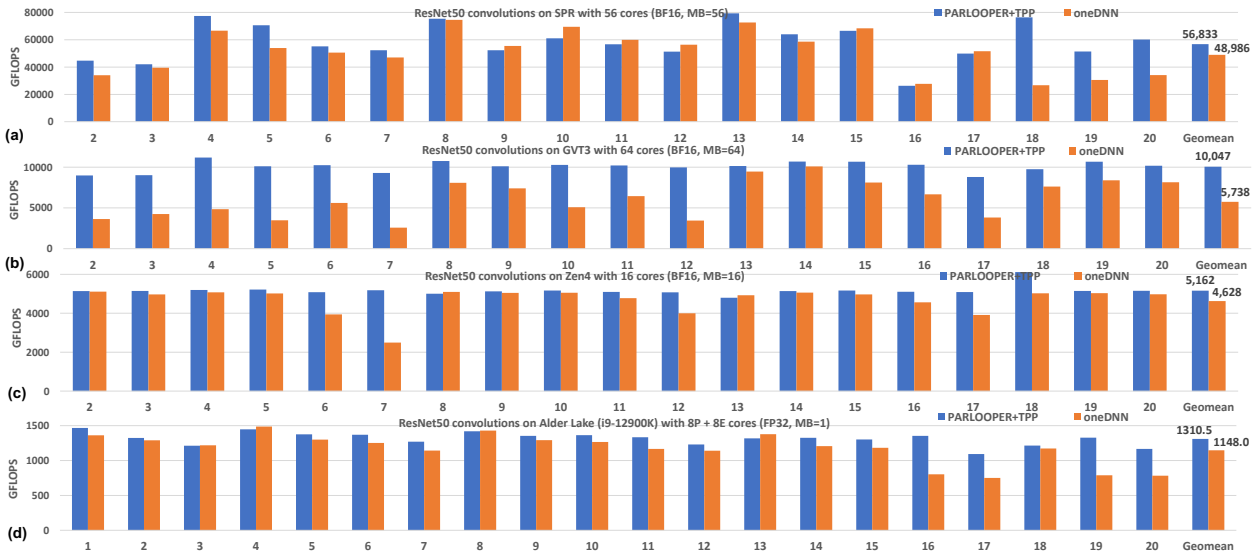
**Table 1: ResNet-50 layers specifications (see Section 3.2).**  $str$  is the stride of the convolution layer.

shows measured performance (left y-axes), and red line shows the modeled performance of the corresponding schedules (right y-axes). Our high-level performance modeling scheme is able to capture the trends pertaining to the various  $loop\_spec\_strings$ : loop instantiations with poor temporal/spatial locality and low-concurrency get a low-score. As a result, the top-5 modeled performant classes (regions that are yellow-shaded in the plots) always contain the most performant loop instantiation candidates, significantly reducing the auto-tuning space. Also, the model refinements mentioned in Section 2.4 should be able to further improve the accuracy of the modelling tool.

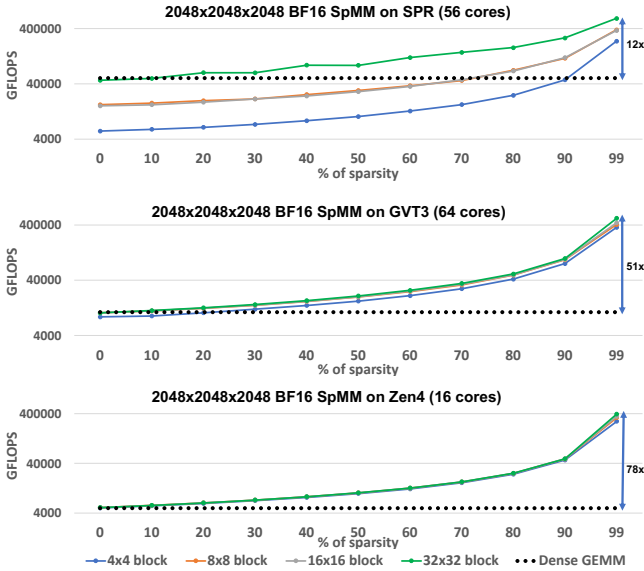
### 5.1.3 Standalone convolution kernels benchmarking

Figure 4 illustrates the PARLOOPER-based implementation of various ResNet50 [22] Convolution layers across all platforms (see Table 1 for the specifications of the convolutions). The minibatch size used on the SPR/GVT3/Zen4 platforms equals to the number of the corresponding cores, whereas on ADL the minibatch is 1 (single-batch inference use-case). We compare the PARLOOPER/TPP implementation (blue bars) against the oneDNN implementation (orange bars). For the first 3 platforms we benchmark BF16 convolutions (SPR, GVT3 and Zen4) whereas on ADL we benchmark FP32 since there is no BF16 hardware support on this platform.

We see that we match/exceed the oneDNN performance across platforms and convolution shapes. By considering the geometric mean on each platform (SPR/GVT3/Zen4/ADL), our implementation outperforms oneDNN by 1.16 $\times$ , 1.75 $\times$ , 1.12 $\times$  and 1.14 $\times$  respectively. For GVT3, the oneDNN/ACL integration is inefficient since it is using the FP32 front-end, and in the backend the input tensors are converted to the BF16 on-the-fly before the actual computation with the BF16-MMLA instructions. Also, we highlight the result on ADL which used both the Performance (P) and Efficiency (E) cores. In our implementation we utilize the *dynamic* OpenMP directive



**Figure 4: Performance of ResNet50 convolution shapes on (a) SPR, (b) GVT3, (c) Zen4, (d) ADL. The x-axis shows the Layer ID (Table 1), the y-axis shows performance in GFLOPS. Blue bars correspond to PARLOOPER/TPP, and orange bars to oneDNN.**



**Figure 5: BF16 Block-SpMM performance ( $M=N=K=2048$ )**

(see Section 2.1), to account for the core heterogeneity and their different compute capabilities. However, we want to emphasize one more time that the convolution code with PARLOOPER/TPP across all platforms and compute-precision is identical to the one in Listing 4: the runtime knob `loop_spec_string` instantiates the surrounding loops in an optimal fashion for the problem/platform at hand, and the BRGEMM TPP dispatches optimal code based on the micro-architecture.

5.1.4 Sparse  $\times$  Dense Matrix-Multiply benchmarking

Figure 5 shows the BF16 Block-SpMM (see Section 3.3) performance of a  $2k \times 2k \times 2k$  Matrix Multiplication on (Top) SPR, (Middle) GVT3, and (Bottom) Zen4. The x-axis represents the sparsity level,

ranging from 0% to 99%, and the y-axis is in logarithmic scale dictating the *effective* GFLOPS. To the best of our knowledge, there is no vendor-optimized library for low-precision block-SpMM, thus we present only PARLOOPER/TPP results. The solid lines correspond to various block-sizes in the block-sparsity structure. As baseline, we show with dashed line the dense GEMM performance on each CPU.

The overall observation is that block-sparsity in conjunction with low-precision FMA acceleration can offer substantial speedups even for modest sparsity levels. More specifically, on SPR and block sizes  $32 \times 32$  we can match the dense GEMM performance even without any sparsity; for 50% sparsity we see 1.7 $\times$  speedup over the dense AMX-accelerated version, and for 99% sparsity we see 12 $\times$  speedup. For block sizes  $16 \times 16$  and  $8 \times 8$  we start seeing benefits from sparsity levels greater than 70%, and for  $4 \times 4$  we only see benefits from extreme sparsity (i.e. greater than 90%). This behavior on SPR is due to the behavior of AMX and the corresponding systolic array: with the larger block sizes, we are able to use efficient two-dimensional AMX tile blocking and fully exploit the systolic array. On the contrary, for smaller block sizes, the “dense” microkernel has small accumulation length which restricts the attainable speedup with AMX. The  $4 \times 4$  case is restricted to  $4/32 = 12.5\%$  of the BF16-compute peak, therefore it requires extreme levels of sparsity to illustrate any benefits.

On GVT3 and Zen4 we start seeing benefits over the dense GEMM kernels even for sparsity levels greater than 10% for all block-sizes (the FMA-BF16 acceleration on these platforms requires accumulation chain of at least 4 and 2 respectively). For GVT3, the maximum attainable speedup with SpMM is 51 $\times$  and for Zen4 it is 78 $\times$  over their relevant dense baselines. These promising results indicate potential speedups for end-to-end workloads, e.g. on BERT inference, where such block-sparsity has shown to work with low precision [36].

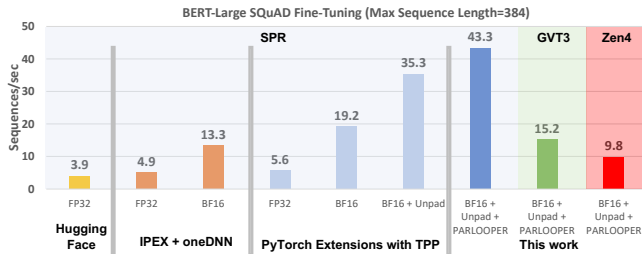


Figure 6: BERT-Large SQuAD Fine-Tuning performance

## 5.2 End-to-end DL Workload Performance

### 5.2.1 Bert Training Results

In Figure 6 we show BERT-Large SQuAD Fine-Tuning [23] performance in Sequences/sec on SPR (blue-shaded area), GVT3 (green shaded area), and Zen4 (red-shaded area). On SPR we compare against alternative implementations: (i) Hugging Face (yellow) [42], (ii) Intel PyTorch Extensions (IPEX) [43] with oneDNN, and (iii) PyTorch Extensions with TPP only [12]. Our implementation extends the open-source code of Georganas et al [12] with PARLOOPER.

First, we observe that the PARLOOPER framework can further speedup the State-Of-The-Art implementation [12] by 1.22 $\times$ . This is achieved by better loop instantiations, which we tuned specifically for the shapes of the workload and resulted in faster tensor contractions. On SPR we observe tensor contraction with average performance of 40 TFLOPS, which is in alignment with our results in Section 5.1.1 (the prior work [12] merely had static loop orders/parallelization in the PyTorch extensions). Our implementation, shows a speedup of 3.3 $\times$  over the Intel PyTorch Extensions (IPEX) [43] with oneDNN, which does *not* use the *Unpad* Optimization that removes unnecessary computations from padded tensors [12]. Our code (Listing 6) is identical across all platforms, and the SPR is 2.8 $\times$  faster than GVT3 and 4.4 $\times$  faster than Zen due to the higher BF16-AMX compute peak of the SPR machine. Last but not least, we want to highlight the fact that our BERT implementation with PARLOOPER/TPP has been adopted by Intel for the recent MLPerf-v2.1 [44] submission (see Table 2) regarding BERT training. The SPR multi-node results (8 and 16 nodes) leverage our implementation with PARLOOPER/TPP, and is integrated with PyTorch Extensions, further highlighting the viability of our framework for real-world, distributed-memory end-to-end production DL workloads. For reference, the 16-node performance is within 2.4 $\times$  from the performance obtained with 8 A100 Nvidia GPUs.

System	Time to train (minutes)
8 nodes SPR (16 sockets)	85.91
16 nodes SPR (32 sockets)	47.26
DGX Box (8xA100 GPU)	19.6

Table 2: Time-to-train performance for BERT. Results from MLPerf-v2.1 (Nov.22) [44]

### 5.2.2 ResNet-50 training Results

Table 3 shows the end-to-end results for ResNet50 BF16-training on a single socket SPR and GVT3 system (Subsection 4.2). We see that the PARLOOPER+TPP implementation is within 4% of the

System	Implementation	Performance in images/sec
GVT3	PARLOOPER + TPP	145
SPR	PARLOOPER + TPP	255
	IPEX + oneDNN	265

Table 3: BF16 training performance of ResNet50 on a single-socket SPR system and on a single socket GVT3.

the Intel PyTorch Extensions (IPEX) [43] with oneDNN. The same code can be readily deployed on GVT3 due to the platform-agnostic nature of PARLOOPER and TPP, yielding performance within 1.76 $\times$  of SPR.

## 6 RELATED WORK

With the rapid development of new DL and HPC workloads, there is a shift to programming paradigms that break the vendor-library performance-portability “jail”. One alternative, “library-free” approach for optimizing DL and HPC kernels is to use modern Tensor Compilers e.g. PlaidML [14], TVM [15], Tensor Comprehensions [16], Ansoor [17], IREE [45]. However, current state-of-the-art tools are only capable of compiling small code blocks while large-scale operators require excessively long compilation, auto-tuning times and frequently result in code that falls short of achieving peak performance [13]. We envision that the high-level loop and tensor abstractions we presented in this work can benefit a tensor compiler infrastructure, e.g. by using the TPP abstraction layer for the ISA-specific backend code generation, and by using the loop instantiation performance modeling in their internal performance models.

Domain Specific Languages (DSLs) have been traditionally used in HPC workloads, and have effectively addressed portability and performance challenges in specific scientific domains [18, 19, 46]. Nevertheless, these DSLs may be considered as point solutions, rather than a universal methodology or paradigm across domains, and they require continuous updates to adapt to the evolving nuances of CPU architectures. To this extend, PARLOOPER could be seen as light-weight library framework for kernel development akin to DSL. However, since the loop-abstraction it provides is generic and high-level, it is not as narrow/task-specific as the majority of the DSLs.

Similar to our approach, but with applicability to GPUs is the CUTLASS [47] framework. It is a collection of CUDA C++ template abstractions for implementing high-performance GEMM and related computations. It decomposes the “moving parts” of tensor contractions into reusable, modular components abstracted by C++ template classes. Primitives at different levels can be specialized and tuned via custom blocking sizes, data types, and other algorithmic strategies. All these high-level ideas are also prevalent in the design philosophy of the PARLOOPER/TPP framework. The Composable Kernel (CK) library [48] aims to provide a programming model for writing performance critical kernels for machine learning workloads targeting multiple architectures (e.g. GPUs and CPUs). It builds on two ideas to attain performance, portability and code maintainability: (i) A tile-based programming model and

(ii) Tensor Coordinate Transformation primitives. The PARLOOP-ER/TPP framework tackles the same problems on CPU platforms via Tensor and Loop high-level abstractions.

## 7 CONCLUSIONS AND FUTURE WORK

In this work we presented a framework to develop efficient, portable DL and HPC kernels for modern CPU architectures. We demonstrate the efficacy of our approach using standalone kernels and end-to-end training DL workloads that outperform state-of-the-art implementations on multiple CPU platforms. As future work, we plan to integrate the standalone kernels we developed in additional end-to-end workloads (e.g. DLRM [31], block-sparse BERT inference [36]). Moreover, we plan to further apply our PARLOOP-ER/TPP kernel development framework on additional CPU architectures (e.g. with RISC-V ISA).

## REFERENCES

- [1] Alex Krizhevsky, I. Sutskever, and G.E. Hinton. Image classification with deep convolutional neural networks. *Advances in neural information processing systems*, pages 1097–1105, 2012.
- [2] Christian Szegedy, Wei Liu, Yangqing Jia, Pierre Sermanet, Scott Reed, Dragomir Anguelov, Dumitru Erhan, Vincent Vanhoucke, and Andrew Rabinovich. Going deeper with convolutions. In *Proceedings of the IEEE conference on computer vision and pattern recognition*, pages 1–9, 2015.
- [3] Karen Simonyan and Andrew Zisserman. Very deep convolutional networks for large-scale image recognition. *arXiv preprint arXiv:1409.1556*, 2014.
- [4] Dong Yu, Michael L Seltzer, Jinyu Li, Jui-Ting Huang, and Frank Seide. Feature learning in deep neural networks—studies on speech recognition tasks. *arXiv preprint arXiv:1301.3605*, 2013.
- [5] Yonghui Wu, Mike Schuster, Zhifeng Chen, Quoc V Le, Mohammad Norouzi, Wolfgang Macherey, Maxim Krikun, Yuan Cao, Qin Gao, Klaus Macherey, et al. Google’s neural machine translation system: Bridging the gap between human and machine translation. *arXiv preprint arXiv:1609.08144*, 2016.
- [6] Heng-Tze Cheng, Levent Koc, Jeremiah Harmsen, Tal Shaked, Tushar Chandra, Hrishikesh Aradhye, Glen Anderson, Greg Corrado, Wei Chai, Mustafa Ispir, et al. Wide & deep learning for recommender systems. In *Proceedings of the 1st Workshop on Deep Learning for Recommender Systems*, pages 7–10. ACM, 2016.
- [7] Thomas Wolf, Julien Chaumond, Lysandre Debut, Victor Sanh, Clement Delangue, Anthony Moi, Pierric Cistac, Morgan Funtowicz, Joe Davison, Sam Shleifer, et al. Transformers: State-of-the-art natural language processing. In *Proceedings of the 2020 Conference on Empirical Methods in Natural Language Processing: System Demonstrations*, pages 38–45, 2020.
- [8] Erik Gawehn, Jan A Hiss, and Gisbert Schneider. Deep learning in drug discovery. *Molecular informatics*, 35(1):3–14, 2016.
- [9] Garrett B Goh, Nathan O Hodas, and Abhinav Vishnu. Deep learning for computational chemistry. *Journal of computational chemistry*, 38(16):1291–1307, 2017.
- [10] Maithra Raghu and Eric Schmidt. A survey of deep learning for scientific discovery. *arXiv preprint arXiv:2003.11755*, 2020.
- [11] Edoardo Angelo Di Napoli, Paolo Bientinesi, Jiajia Li, and André Uchsmajew. High-performance tensor computations in scientific computing and data science. *Frontiers in Applied Mathematics and Statistics*, page 93, 2022.
- [12] Evangelos Georganas, Dhiraj Kalamkar, Sasikanth Avancha, Menachem Adelman, Cristina Anderson, Alexander Breuer, Jeremy Bruestle, Narendra Chaudhary, Abhisek Kundu, Denise Kutnick, et al. Tensor processing primitives: A programming abstraction for efficiency and portability in deep learning workloads. In *Proceedings of the International Conference for High Performance Computing, Networking, Storage and Analysis*, pages 1–14, 2021.
- [13] Paul Barham and Michael Isard. Machine learning systems are stuck in a rut. In *Proceedings of the Workshop on Hot Topics in Operating Systems*, pages 177–183, 2019.
- [14] Tim Zerrell and Jeremy Bruestle. Stripe: Tensor compilation via the nested polyhedral model. *arXiv preprint arXiv:1903.06498*, 2019.
- [15] Tianqi Chen, Thierry Moreau, Ziheng Jiang, Lianmin Zheng, Eddie Yan, Haichen Shen, Meghan Cowan, Leyuan Wang, Yuwei Hu, Luis Ceze, et al. {TVM}: An automated end-to-end optimizing compiler for deep learning. In *13th {USENIX} Symposium on Operating Systems Design and Implementation ({OSDI} 18)*, pages 578–594, 2018.
- [16] Nicolas Vasilache, Oleksandr Zinenko, Theodoros Theodoridis, Priya Goyal, Zachary DeVito, William S Moses, Sven Verdoolaege, Andrew Adams, and Albert Cohen. Tensor comprehensions: Framework-agnostic high-performance machine learning abstractions. *arXiv preprint arXiv:1802.04730*, 2018.
- [17] Lianmin Zheng, Chengfan Jia, Minmin Sun, Zhao Wu, Cody Hao Yu, Ameer Haj-Ali, Yida Wang, Jun Yang, Danyang Zhuo, Koushik Sen, et al. Anso: Generating high-performance tensor programs for deep learning. In *14th {USENIX} Symposium on Operating Systems Design and Implementation ({OSDI} 20)*, pages 863–879, 2020.
- [18] Nathan Zhang, Michael Driscoll, Charles Markley, Samuel Williams, Protonu Basu, and Armando Fox. Snowflake: a lightweight portable stencil dsl. In *2017 IEEE International Parallel and Distributed Processing Symposium Workshops (IPDPSW)*, pages 795–804. IEEE, 2017.
- [19] Jonathan Ragan-Kelley, Connelly Barnes, Andrew Adams, Sylvain Paris, Frédo Durand, and Suman Amarasinghe. Halide: a language and compiler for optimizing parallelism, locality, and recomputation in image processing pipelines. *Acm Sigplan Notices*, 48(6):519–530, 2013.
- [20] Evangelos Georganas, Sasikanth Avancha, Kunal Banerjee, Dhiraj Kalamkar, Greg Henry, Hans Pabst, and Alexander Heinecke. Anatomy of high-performance deep learning convolutions on SIMD architectures. In *Proceedings of the International Conference for High Performance Computing, Networking, Storage, and Analysis*, page 66. IEEE Press, 2018.
- [21] Evangelos Georganas, Kunal Banerjee, Dhiraj Kalamkar, Sasikanth Avancha, Anand Venkat, Michael Anderson, Greg Henry, Hans Pabst, and Alexander Heinecke. Harnessing deep learning via a single building block. In *2020 IEEE International Parallel and Distributed Processing Symposium (IPDPS)*, pages 222–233. IEEE, 2020.
- [22] Kaiming He, Xiangyu Zhang, Shaoqing Ren, and Jian Sun. Deep residual learning for image recognition. In *Proceedings of the IEEE conference on computer vision and pattern recognition*, pages 770–778, 2016.
- [23] Jacob Devlin, Ming-Wei Chang, Kenton Lee, and Kristina Toutanova. Bert: Pre-training of deep bidirectional transformers for language understanding. *arXiv preprint arXiv:1810.04805*, 2018.
- [24] Rohit Chandra, Leo Dagum, Ramesh Menon, David Kohr, Dror Maydan, and Jeff McDonald. *Parallel programming in OpenMP*. Morgan kaufmann, 2001.
- [25] Chuck Pheatt. Intel® threading building blocks. *Journal of Computing Sciences in Colleges*, 23(4):298–298, 2008.
- [26] Bradford Nichols, Dick Buttlar, Jacqueline Farrell, and Jackie Farrell. *Pthreads programming: A POSIX standard for better multiprocessing*. " O'Reilly Media, Inc.", 1996.
- [27] Kazushige Goto and Robert A Geijn. Anatomy of high-performance matrix multiplication. *ACM Transactions on Mathematical Software (TOMS)*, 34(3):12, 2008.
- [28] Jason Ansel, Shoaib Kamil, Kalyan Veeramachaneni, Jonathan Ragan-Kelley, Jeffrey Bosboom, Una-May O’Reilly, and Suman Amarasinghe. Opentuner: An extensible framework for program autotuning. In *Proceedings of the 23rd international conference on Parallel architectures and compilation*, pages 303–316, 2014.
- [29] Sanket Tavarageri, Alexander Heinecke, Sasikanth Avancha, Bharat Kaul, Gagan-deep Goyal, and Ramakrishna Upadrastra. Polydl: Polyhedral optimizations for creation of high-performance dl primitives. *ACM Transactions on Architecture and Code Optimization (TACO)*, 18(1):1–27, 2021.
- [30] Tom Brown, Benjamin Mann, Nick Ryder, Melanie Subbiah, Jared D Kaplan, Prafulla Dhariwal, Arvind Neelakantan, Pranav Shyam, Girish Sastry, Amanda Askell, et al. Language models are few-shot learners. *Advances in neural information processing systems*, 33:1877–1901, 2020.
- [31] Maxim Naumov, Dheevatsa Mudigere, Hao-Jun Michael Shi, Jianyu Huang, Narayanan Sundaraman, Jongsoo Park, Xiaodong Wang, Udit Gupta, Carole-Jean Wu, Alisson G Azzolini, et al. Deep learning recommendation model for personalization and recommendation systems. *arXiv preprint arXiv:1906.00091*, 2019.
- [32] Alexander Heinecke, Greg Henry, Maxwell Hutchinson, and Hans Pabst. LIBXSMM: Accelerating small matrix multiplications by runtime code generation. In *Proceedings of the International Conference for High Performance Computing, Networking, Storage and Analysis*, SC ’16, pages 84:1–84:11, Piscataway, NJ, USA, 2016. IEEE Press.
- [33] Nigel Stephens, Stuart Biles, Matthias Boettcher, Jacob Eapen, Mbou Eyole, Giacomo Gabrielli, Matt Horsnell, Grigorios Magklis, Alejandro Martinez, Nathanael Premillieu, et al. The arm scalable vector extension. *IEEE micro*, 37(2):26–39, 2017.
- [34] Md Mostofa Ali Patwary, Nadathur Rajagopalan Satish, Narayanan Sundaram, Jongsoo Park, Michael J Anderson, Satya Gautam Vadlamudi, Dipankar Das, Sergey G Pudov, Vadim O Pirogov, and Pradeep Dubey. Parallel efficient sparse matrix-matrix multiplication on multicore platforms. In *High Performance Computing: 30th International Conference, ISC High Performance 2015, Frankfurt, Germany, July 12–16, 2015, Proceedings*, pages 48–57. Springer, 2015.
- [35] Torsten Hoefler, Dan Alistarh, Tal Ben-Nun, Nikoli Dryden, and Alexandra Peste. Sparsity in deep learning: Pruning and growth for efficient inference and training in neural networks. *The Journal of Machine Learning Research*, 22(1):10882–11005, 2021.
- [36] François Lagunas, Ella Charlaix, Victor Sanh, and Alexander M Rush. Block pruning for faster transformers. *arXiv preprint arXiv:2109.04838*, 2021.

- [37] Thomas Wolf, Lysandre Debut, Victor Sanh, Julien Chaumond, Clement Delangue, Anthony Moi, Pierric Cistac, Tim Rault, R Almi Louf, Morgan Funtowicz, Joe Davison, Sam Shleifer, Patrick von Platen, Clara Ma, Yacine Jernite, Julien Plu, Canwen Xu, Teven Le Scao, Sylvain Gugger, Mariama Drame, Quentin Lhoest, and Alexander M. Rush. Transformers: State-of-the-art natural language processing. In *Proceedings of the 2020 Conference on Empirical Methods in Natural Language Processing: System Demonstrations*, pages 38–45, Online, October 2020. Association for Computational Linguistics.
- [38] Kunal Banerjee, Evangelos Georganas, Dhiraj D Kalamkar, Barukh Ziv, Eden Segal, Cristina Anderson, and Alexander Heinecke. Optimizing deep learning rnn topologies on intel architecture. *Supercomputing Frontiers and Innovations*, 6(3):64–85, 2019.
- [39] Minjia Zhang, Samyam Rajbhandari, Wenhan Wang, and Yuxiong He. Deepcpu: Serving rnn-based deep learning models 10x faster. In *2018 {USENIX} Annual Technical Conference ({USENIX} {ATC} 18)*, pages 951–965, 2018.
- [40] Intel oneDNN. <https://github.com/oneapi-src/onednn>, Accessed on 4/6/2023.
- [41] ARM. <https://github.com/arm-software/computelibrary>, Accessed on 4/6/2023.
- [42] Hugging Faces. <https://github.com/huggingface/transformers>, Accessed on 4/6/2023.
- [43] Intel Extension for PyTorch. <https://github.com/intel/intel-extension-for-pytorch>, Accessed on 4/6/2023.
- [44] ML Commons. <https://mlcommons.org/en/training-normal-21/>, Accessed on 4/6/2023.
- [45] IREE. <https://github.com/openxla/iree>, Accessed on 4/6/2023.
- [46] Ivens Portugal, Paulo Alencar, and Donald Cowan. A survey on domain-specific languages for machine learning in big data. *arXiv preprint arXiv:1602.07637*, 2016.
- [47] Vijay Thakkar, Pradeep Ramani, Cris Cecka, Aniket Shivam, Honghao Lu, Ethan Yan, Jack Kosaian, Mark Hoemmen, Haicheng Wu, Andrew Kerr, Matt Nicely, Duane Merrill, Dustyn Blasig, Fengqi Qiao, Piotr Majcher, Paul Springer, Markus Hohnerbach, Jin Wang, and Manish Gupta. CUTLASS, 1 2023.
- [48] Chao Liu, Jing Zhang, Letao Qin, Qianfeng Zhang, Liang Huang, Shaojie Wang, Anthony Chang, Chunyu Lai, Illia Silin, Adam Osewski, Poyen Chen, Rosty Geyyer, Hanwen Chen, Tejash Shah, Xiaoyan Zhou, and Jianfeng Yan. Composable Kernel.
- Optimization Notice: Software and workloads used in performance tests may have been optimized for performance only on Intel microprocessors. Performance tests, such as SYSmark and MobileMark, are measured using specific computer systems, components, software, operations and functions. Any change to any of those factors may cause the results to vary. You should consult other information and performance tests to assist you in fully evaluating your contemplated purchases, including the performance of that product when combined with other products. For more information go to <http://www.intel.com/performance>.
- Intel, Xeon, and Intel Xeon Phi are trademarks of Intel Corporation in the U.S. and/or other countries.